

Use of Monte Carlo calculations in the study of microtubule subunit kinetics

(GTP cap/nonlinear flux/steady state/transient)

YI-DER CHEN AND TERRELL L. HILL

Laboratory of Molecular Biology, National Institute of Arthritis, Diabetes, and Digestive and Kidney Diseases, National Institutes of Health, Building 2, Room 317, Bethesda, MD 20205

Contributed by Terrell L. Hill, May 31, 1983

ABSTRACT GTP-tubulin forms a cap on microtubule ends during aggregation. The bulk of the microtubule is GDP-tubulin. This complicates the usual simple kinetic theory of subunit exchange at microtubule ends to such an extent that Monte Carlo calculations are needed to handle the complications, except in special cases. The Monte Carlo method is introduced here, for this problem, and illustrated with steady-state and transient examples. Monte Carlo transients are needed to simulate dilution experiments. Preliminary results (with M. F. Carlier) have been obtained applying these theoretical procedures to experimental data.

There is evidence (1) that GTP-tubulin (called T, below) forms a steady-state cap at and near an end of a microtubule, though in the deep interior the subunits of the polymer are all GDP-tubulin (called D, below). Until recently, it was thought that an added T hydrolyzes very quickly to D at the very tip of a microtubule so that the entire polymer would consist of, for practical purposes, D units only. In the newer view (1, 2), a given T unit that adds to the tip might be buried in the microtubule end but would eventually become D, if it does not first leave. In steady-state growth (or even steady shortening), there would then be a certain statistical population of still surviving T near the end of the microtubule—the GTP cap.

The steady-state kinetic theory of microtubule and actin polymerization (3, 4) therefore needs modification, at least for microtubules—and probably also for actin (5, 6). An attempt at this was made in ref. 4, where the five helices (assuming a five-start helix) of a microtubule were assumed to be independent of each other and an “uncorrelated approximation” was then used in the treatment of a single independent helix. The next step (7) was to give an exact analytical treatment of the problem that avoided the uncorrelated approximation but that had to be limited to the special case (see Fig. 1) $\kappa = 0$, $\alpha_{1D} = 0$, except near $c = 0$ (c is the concentration of free T). Because the experimental values of κ and α_{1D} are both believed to be small, this treatment is probably fairly realistic. An interesting result was that the theory predicted a significant discontinuity in slope for the steady-state subunit flux as a function of c , at the critical concentration (where flux = 0).

The purpose of the present paper is to introduce the Monte Carlo method for this problem and to present a few illustrative properties of the system. With this approach, we are no longer limited to the special case $\kappa = 0$, $\alpha_{1D} = 0$. In fact, the assumption of independent helices could also be avoided by the Monte Carlo method, but we do not include that more elaborate step here. Instead, we treat an independent helix (or “polymer”), with arbitrary rate constants, at steady state. In work with M. F. Carlier, we have obtained preliminary results using

the present Monte Carlo formulation in an attempt to fit experimental flux–concentration curves (8). This fitting involves not only steady-state properties but also Monte Carlo transients that simulate experimental dilution experiments. We discuss Monte Carlo transients briefly in the final section.

THE MODEL AND METHOD

Fig. 1*a* shows the types of transitions that are included in the model for the α end of the polymer (7). The rate constants κ (interior; $n \geq 2$) and κ' (tip only; $n = 1$) both refer to hydrolysis of GTP to GDP, whereas κ'' refers to exchange of GTP for GDP on an end ($n = 1$) subunit only. The “on” rate constant α_1 (the only second-order rate constant) in Fig. 1*a* is actually subdivided, in our model, as shown in Fig. 1*b*. That is, the value of this rate constant depends on the receiving subunit; experimentally (9), α_{1D} is much smaller than α_{1T} but we do not concern ourselves with this limitation in the present paper on methodology. The two “off” rate constants in Fig. 1*a* are also subdivided, as shown in Fig. 1*c*. In this case, the neighbor at position $n = 2$ may make a difference (however, in the numerical examples here, we take $\alpha_{2D} = \alpha_{2T}$ and $\alpha_{-1D} = \alpha_{-1T}$). Exchange of GTP for GDP is assumed to be very fast in solution, so only T (concentration, c) is present there.

In a Monte Carlo calculation (10), we start ($t = 0$) with a single polymer in a particular state, say all D,



and follow its stochastic history in detail through many transitions. As an example, the possible transitions from this particular initial state are (Fig. 1) κ'' , α_{2D} , and $\alpha_{1D}c$. The time spent in this state, used in calculating time averages later, is taken to be the mean lifetime

$$(\kappa'' + \alpha_{2D} + \alpha_{1D}c)^{-1}.$$

A distribution of lifetimes can easily be used instead of the mean lifetime, but this is an unnecessary refinement for steady-state calculations (see, however, the last section). The transition that takes place after the mean lifetime may be any one of the three mentioned above. The probability that it is, say, the κ'' transition is

$$\kappa'' / (\kappa'' + \alpha_{2D} + \alpha_{1D}c),$$

with similar expressions for the other two probabilities. Taking into account these three probabilities, a random-number generator in the computer selects the actual transition that occurs, leading to the next state. If, in this example, the transition happens to be α_{2D} , then the polymer is still in the all-D state. In this case, the second transition would be handled just like the first transition. However, if the first transition is κ'' or $\alpha_{1D}c$, the second state in the sequence is



The publication costs of this article were defrayed in part by page charge payment. This article must therefore be hereby marked “advertisement” in accordance with 18 U.S.C. §1734 solely to indicate this fact.

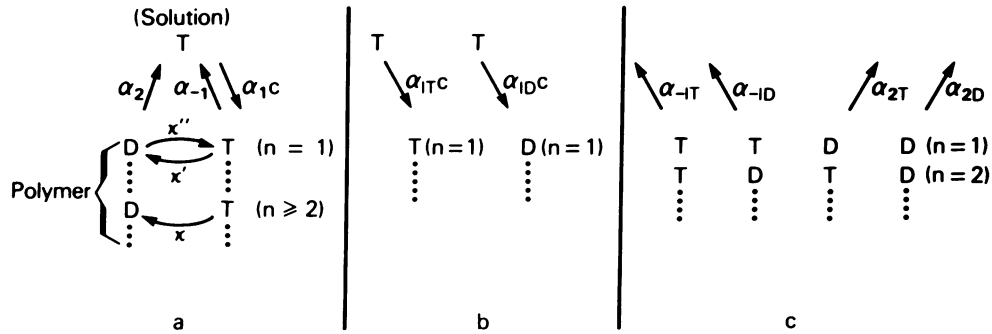


FIG. 1. (a) Types of transitions included in the model. (b) Subdivision of α_1 according to occupant of position $n = 1$. (c) Subdivision of α_1 and α_2 according to occupant of position $n = 2$.

The possible transitions out of this state are (Fig. 1) κ' , α_{-1D} , and α_{1Tc} . The mean lifetime in this state is

$$(\kappa' + \alpha_{-1D} + \alpha_{1Tc})^{-1}.$$

The probability that the transition out of this state is, say, κ' is

$$\kappa' / (\kappa' + \alpha_{-1D} + \alpha_{1Tc}),$$

etc. Again a random number is used to select a particular transition from among the three possibilities.

The above procedure is repeated for a very large number of transitions. The computer keeps a record of the sequence of states and of the mean lifetime of each state. Time averages for this one polymer (rather than an ensemble average over many polymers) are then calculated for the various quantities of interest, each state being weighted, in calculating these averages, by its mean lifetime. The computation of averages is started only after a discard of (usually) 10^4 transitions to allow the system to reach steady state. Most points in Fig. 2 are based on 2×10^5 transitions, though some (smaller c values) are for 10^5 transitions and a few are for 10^6 transitions. The subunit flux J_a (mean rate of addition of subunits) and the mean rate of GTP hydrolysis J_h are calculated indirectly from time-averaged probabilities rather than by direct counting. This indirect method

is more accurate (11) for the mean values but it would not be suitable if fluctuations in the two fluxes were of interest. Direct counting is used for transients (last section). Specifically, we use

$$J_a = \alpha_{1Tc}p_1 + \alpha_{1Dc}(1 - p_1) - \alpha_{2D}p_{DD} - \alpha_{2T}p_{DT} - \alpha_{-1D}p_{TD} - \alpha_{-1T}p_{TT} \quad [1]$$

and

$$J_h = \alpha_{1Tc}p_1 + \alpha_{1Dc}(1 - p_1) + \kappa''(1 - p_1) - \alpha_{-1D}p_{TD} - \alpha_{-1T}p_{TT}, \quad [2]$$

where p_n is the probability that position n is in state T (rather than D), p_{DD} is the probability that positions $n = 1, 2$ are in the particular dual state DD, etc. An alternative calculation of J_h that is used as a check is

$$J_h = \kappa'p_1 + \kappa \sum_{n \geq 2} p_n. \quad [3]$$

The meaning of the terms in Eqs. 1 and 3 are obvious from Fig. 1. Whereas Eq. 3 gives the steady-state rate of disappearance of T from the polymer by hydrolysis, Eq. 2 gives the net steady-

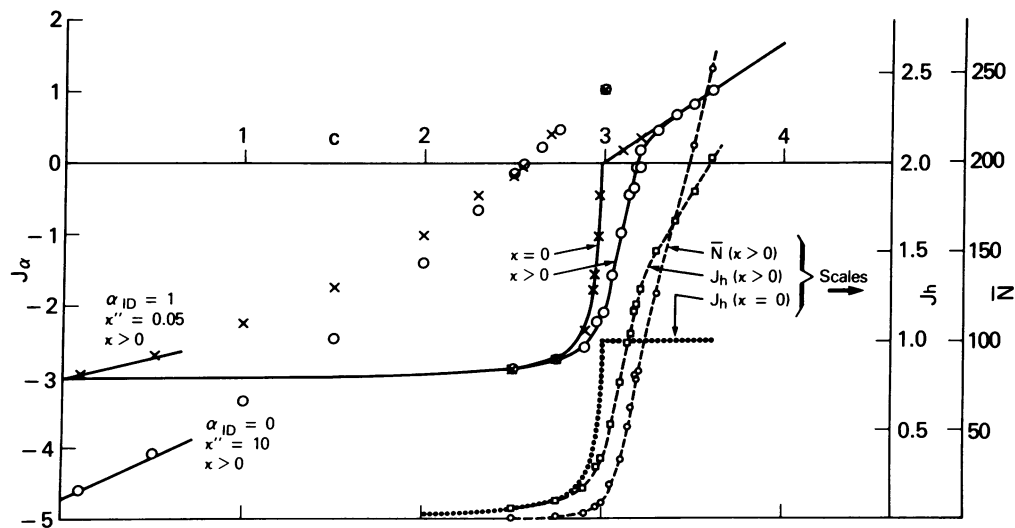


FIG. 2. Illustrative Monte Carlo steady-state calculations. The full solid curve (—) labeled $\kappa = 0$ is exact and calculated analytically. Points on this curve are Monte Carlo points, which serve as a check of the Monte Carlo program. The adjacent solid curve (○—○) labeled $\kappa > 0$ is a smooth curve through Monte Carlo points. The dotted curve (·····) directly below is the exact $\kappa = 0$ J_h curve. The adjacent dashed curves (□---□ and ○---○) are Monte Carlo curves ($\kappa > 0$) for J_h and N . The short lines near $c = 0$ are exact in the limit $c \rightarrow 0$ for the parameters given in the figure. The associated points (extended to larger c) are Monte Carlo points for the same cases.

state rate at which T is added to the polymer by all other transition types. The two rates (Eqs. 2 and 3) should be equal at steady state because the total T in the polymer is constant at steady state. Of course, in a Monte Carlo calculation they will not be exactly equal, because of fluctuations.

If, to be precise, we define (7) the GTP cap as consisting of all those Ts in interior positions $n = 2, 3, \dots$, then the mean number of Ts in the cap at steady state is easily found from the time-averaged p_n values as

$$\bar{N} = \sum_{n=2} p_n. \quad [4]$$

RESULTS

In ref. 7, exact analytical expressions were derived for the cases (i) $\kappa = 0$, $\alpha_{1D} = 0$ at any c and (ii) $c \rightarrow 0$ for any κ and α_{1D} . These expressions will not be repeated here. The solid curve in Fig. 2 labeled $\kappa = 0$, with discontinuity in slope at $J_\alpha = 0$, $c = c_\alpha$, is the exact $J_\alpha(c)$ for the reference case (7)

$$\begin{aligned} \kappa = 0, \kappa' = 1.5, \kappa'' = 0.05, \alpha_{1T} = 2.5, \alpha_{1D} = 0 \\ \alpha_{-1T} = 6, \alpha_{-1D} = 6, \alpha_{2T} = 3, \alpha_{2D} = 3. \end{aligned} \quad [5]$$

The units are s^{-1} except $\mu M^{-1}s^{-1}$ for α_{1T} and α_{1D} ; the units for c are μM . The points (\times) on this curve are Monte Carlo J_α points for the same case, thus providing a check on our procedure. The corresponding analytical curve for J_h is the dotted curve, with ordinate shown on the right of the figure. In this case, when $J_\alpha > 0$ ($c > c_\alpha = 2.99 \mu M$), the T cap grows at a steady rate and has no definite steady size (because $\kappa = 0$). Correspondingly, J_h is constant when $J_\alpha > 0$. In fact, in this case, $J_h = \kappa' p_1$ and p_1 is constant at the value 0.6703 for $c \geq c_\alpha$.

The solid curve in Fig. 2 labeled $\kappa > 0$ is a smooth curve drawn through Monte Carlo points (\circ) for the reference case modified only by taking $\kappa = 0.25/60 s^{-1}$ (i.e., $\kappa = 0.25 \text{ min}^{-1}$), which is an experimental value (1). In fact, all curves in Fig. 2 labeled $\kappa > 0$ are for this same small value of κ . This small change in κ (i.e., from 0 to 0.25 min^{-1}) is seen to have a very large effect on J_α in the neighborhood of $c = c_\alpha$. However, this effect disappears on either side of $c = c_\alpha$ (i.e., the two solid curves converge). This large sensitivity of J_α to a small κ near $c = c_\alpha$ arises because κ'' is very small in this case, $\kappa'' = 0.05$. As shown in ref. 7, a small κ'' leads to an almost vertical J_α just below $c = c_\alpha$ when $\kappa = 0$. As we shall see below, this effect of small κ on J_α is hardly noticeable when $\kappa'' = 10$.

The two dashed curves (right-hand scales) in Fig. 2 are for this same case ($\kappa > 0$): one curve gives $J_h(c)$ and the other gives $\bar{N}(c)$. Both curves have a break in slope at about $c = c_\alpha \approx 3.19 \mu M$.

Table 1 also relates to this case. Columns 2, 3, and 4 are Monte Carlo results (with $\kappa > 0$) for $c > c_\alpha$. These numbers are, of course, subject to fluctuations. Column 5 gives the exact analytical J_α for $\kappa = 0$ (the Eq. 5 case), denoted J_α^0 in Table 1. J_α is close to J_α^0 for $c \geq 3.4$ (as is also evident in Fig. 2). The last column in Table 1 gives J_α^0/κ , which is a good approximation to \bar{N} when $\kappa > 0$, as pointed out in ref. 7. Note in Table 1 that

Table 1. Some Monte Carlo results for $\kappa'' = 0.05$, $\kappa > 0$

| c | Monte Carlo ($\kappa > 0$) | | | J_α^0 ($\kappa = 0$) | J_α^0/κ |
|-----|------------------------------|-----------|---------|----------------------------------|---------------------|
| | J_α | \bar{N} | p_2 | | |
| 3.3 | 0.4537 | 126.8 | 0.98788 | 0.5192 | 124.6 |
| 3.4 | 0.6674 | 167.2 | 0.99214 | 0.6868 | 164.8 |
| 3.5 | 0.8167 | 209.0 | 0.99456 | 0.8544 | 205.1 |
| 3.6 | 1.0221 | 253.2 | 0.99598 | 1.0220 | 245.3 |

Table 2. Some Monte Carlo results for $\kappa'' = 10$, $\kappa > 0$

| c | J_α , MC ($\kappa > 0$) | J_α^0 ($\kappa = 0$) | Δ |
|------|-------------------------------------|----------------------------------|----------|
| 0.10 | -4.5995 | -4.5942 | 0.005 |
| 0.50 | -4.0764 | -4.0769 | 0.000 |
| 1.00 | -3.3334 | -3.3333 | 0.000 |
| 1.50 | -2.4553 | -2.4545 | 0.001 |
| 2.00 | -1.4040 | -1.4000 | 0.004 |
| 2.30 | -0.6688 | -0.6596 | 0.009 |
| 2.50 | -0.1430 | -0.1111 | 0.032 |
| 2.55 | -0.0162 | 0.0259 | 0.042 |
| 2.65 | 0.2265 | 0.2500 | 0.024 |
| 2.75 | 0.4634 | 0.4741 | 0.011 |
| 3.00 | 1.0305 | 1.0345 | 0.004 |

p_2 is close to unity for $c \geq 3.4$. When $\kappa = 0$, p_2 is exactly unity for $J_\alpha > 0$ (7).

Another case included in Fig. 2 modifies the reference case (Eq. 5) by taking $\kappa'' = 10$ and $\kappa = 0.25 \text{ min}^{-1}$. With this large value of κ'' , a small κ has almost no effect on J_α , even near $c = c_\alpha$. The points (\circ) labeled $\alpha_{1D} = 0$, $\kappa'' = 10$, $\kappa > 0$ are Monte Carlo J_α values. The associated (lower) short solid line is the exact behavior (7) of J_α near $c = 0$ for this case. Note that the discontinuity in slope at $c = c_\alpha$ is no longer evident (7). Table 2 compares $\kappa > 0$ Monte Carlo values of J_α with the exact J_α when $\kappa = 0$ (denoted J_α^0). That is, the J_α^0 values correspond to the Eq. 5 reference case except that $\kappa'' = 10$. Δ in Table 2 is the difference, $J_\alpha^0 - J_\alpha$; it is small everywhere (i.e., κ has little effect on J_α) but reaches a maximum near $c = c_\alpha$, just as in the $\kappa'' = 0.05$ case discussed above (see the two solid curves in Fig. 2).

The last case included in Fig. 2 is labeled $\alpha_{1D} = 1$, $\kappa'' = 0.05$, $\kappa > 0$. This is the Eq. 5 reference case except for $\alpha_{1D} = 1$ and $\kappa = 0.25 \text{ min}^{-1}$. Presumably the change in κ (from $\kappa = 0$) is insignificant and this case mainly shows the effect of a non-zero α_{1D} . The Monte Carlo points (\times) again do not exhibit a discontinuity in slope at $c = c_\alpha$. The upper short solid line indicates, as before, the exact behavior (7) near $c = 0$. The fact that both short solid lines have significant slope at $c = 0$ (in contrast to the reference case) is due to $\alpha_{1D} = 1$ in one case and $\kappa'' = 10$ in the other. These rate constants relate to mechanisms (Fig. 1) that allow T from solution to attach to the polymer end when c is very small (7).

Finally, we mention that the uncorrelated approximation is found to be satisfactory in all these cases when $J_\alpha > 0$ but not otherwise. We therefore conclude that, unfortunately, the uncorrelated approximation is of little value for this problem.

MONTE CARLO TRANSIENTS

To simulate a dilution experiment (8), we start with a Monte Carlo simulation of the steady state for one polymer molecule at $c = c_\alpha$, typically over 3×10^5 transitions, using the procedure described above. At $t = 0$, the free subunit concentration is changed from $c = c_\alpha$ to any c value, say $c = c'$. The object then is to obtain $J_\alpha(t)$ after the jump in c , holding $c = c'$ constant. In the corresponding experiment, however, c does not remain constant at c' . Hence, our primary interest here—for comparison with experiment—is in early times, before the experimental c' changes significantly.

The procedure we use to calculate $J_\alpha(t)$, for $t > 0$, is to follow an ensemble of, typically, 10^4 Monte Carlo polymers, starting at $t = 0$, and record the ensemble averaged net gain or loss of subunits per polymer in successive small time intervals, starting at $t = 0$. For each polymer, the gain or loss is actually counted; Eq. 1 is not used. The ensemble is selected from the 3×10^5

sequence of states in the steady-state simulation. That is, after every $3 \times 10^5/10^4 = 30$ transitions in the steady state, a polymer state is chosen for the subsequent ensemble averaging with $t > 0$.

Thus, in the steady state, we use long-time averaging for one polymer, but in the transient ($t > 0$) we switch to ensemble averaging over many polymers (because properties are changing with time). Each of the 10^4 states or polymers selected for the ensemble from the 3×10^5 sequence of states in the steady state has a certain mean lifetime, already discussed above. This mean lifetime of a particular polymer must be used as a constant weight for this polymer, as it evolves, in calculating ensemble averages for $t > 0$. This is equivalent to including in the ensemble a number of replicas of the polymer state proportional to the mean lifetime of the state. If this is not done, time averaging and ensemble averaging will not be equivalent.

It is also necessary, in following the stochastic history of each polymer in the ensemble, during $t > 0$, to use a random time distribution rather than the mean lifetime as the waiting time between transitions. Specifically, for a particular polymer in the ensemble in a particular state, with a mean lifetime \bar{t} (equal to the reciprocal of the sum of rate constants for all possible transitions while in the given state), the waiting time until the next transition is

$$t = \bar{t} \ln R^{-1}, \quad [6]$$

where R is a random number uniformly distributed between 0 and 1.

The initial subunit flux in the transient—i.e., $J_\alpha(0)$ after $c = c_\alpha$ is suddenly changed to $c = c'$ at $t = 0$ —can be calculated directly from steady-state properties; the transient itself is not needed to find this starting point. The transient, however, provides a self-consistency check. In Eq. 1, for the $c = c_\alpha$ steady state, all of the p values are appropriate to c_α . At $c = c_\alpha$, we rewrite Eq. 1 as

$$J_\alpha^{ss} = [\alpha_{1T}p_1^{ss} + \alpha_{1D}(1 - p_1^{ss})]c_\alpha - [\alpha_{2D}p_{DD}^{ss} + \alpha_{2T}p_{DT}^{ss} + \alpha_{1D}p_{TD}^{ss} + \alpha_{1T}p_{TT}^{ss}], \quad [7]$$

where the superscript *ss* refers to the $c = c_\alpha$ steady state. Of course, J_α^{ss} will be virtually zero but not exactly zero because of fluctuations in the Monte Carlo steady-state calculation. In addition, the value to use for c_α itself (defined by $J_\alpha = 0$) is not known precisely. After the instantaneous jump to $c = c'$ at $t = 0$, the left-hand side of Eq. 7 becomes $J_\alpha(0)$, and on the right-hand side c_α is replaced by c' . There is no other change on the right-hand side: the p values have not started yet to change with time. On combining these two equations, we have

$$J_\alpha(0) = J_\alpha^{ss} + [\alpha_{1T}p_1^{ss} + \alpha_{1D}(1 - p_1^{ss})](c' - c_\alpha). \quad [8]$$

Thus, $J_\alpha(0)$ is a linear function of c' , with slope [] and intercept, at $c' = 0$, $-c_\alpha$ [] (neglecting J_α^{ss}).

Fig. 3 presents an example. Starting with the $c = c_\alpha = 3.19 \mu\text{M}$ steady state in Fig. 2 (solid curve, $\kappa > 0$), using 3×10^5 transitions, the system is jumped to $c' = 2.5 \mu\text{M}$ and the transient is followed with an ensemble of 10^4 polymers. From $J_\alpha^{ss} = -0.0061 \text{ s}^{-1}$ and $p_1^{ss} = 0.6018$, Eq. 8 gives $J_\alpha(0) = -1.044 \text{ s}^{-1}$ at $c' = 2.5 \mu\text{M}$. At $t = \infty$, $J_\alpha(\infty) = -2.89 \text{ s}^{-1}$. This is the steady-state value of J_α at $c = 2.5 \mu\text{M}$ (Fig. 2). Fig. 3 shows $J_\alpha(t)$ from the Monte Carlo transient calculation. The individual points (○) were obtained by counting on and off subunit tran-

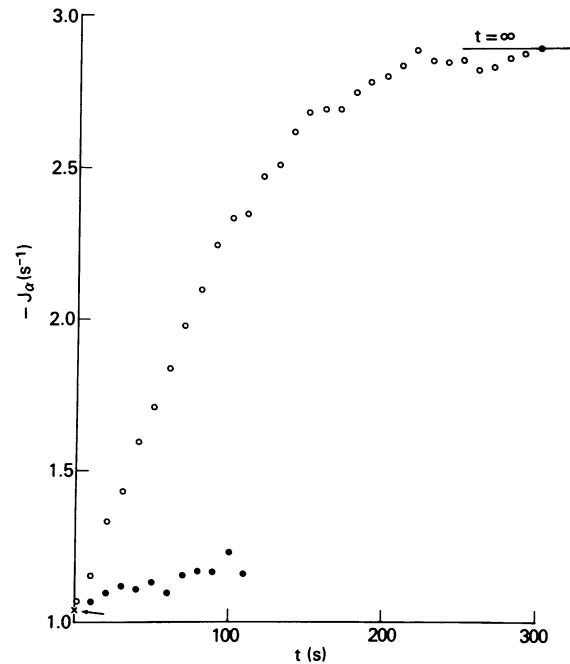


FIG. 3. Illustrative Monte Carlo transient in which the $c = c_\alpha = 3.19 \mu\text{M}$ steady state is jumped to $c = c' = 2.5 \mu\text{M}$. The arrow points at $-J_\alpha(0) = -1.044 \text{ s}^{-1}$ (○).

sitions in the 10^4 polymers over a time interval of 1 s. Only every 10th such point is included in the figure ($t = 1, 11, 21, \dots$). The steady-state values of $J_\alpha(0)$ (arrow) and $J_\alpha(\infty)$ ($t = \infty$ line) are confirmed by the transient. The points at the bottom (●) are on a different time scale (100 s \rightarrow 10 s). They are the points for $t = 1, 2, \dots, 11$ s.

In a dilution experiment, there is a dead time after mixing of order 3–5 s before a measurement is made. The theoretical quantity of interest is therefore not $J_\alpha(0)$ but something like $J_\alpha(4 \text{ s})$. In this unrealistic example (Fig. 3), there is very little change in $J_\alpha(t)$ by $t = 4$ s.

To increase the rate at which the T cap is lost from the steady-state polymer when c_α is jumped to $c' < c_\alpha$, we have also included in the Monte Carlo program the possibility of cooperativity in the cap. This is accomplished by using four different κ values for Ts in positions $n = 2, 3, \dots$, according as the nearest neighbors of a T in any of these positions are DD, DT, TD, or TT. If only the DD and TD cases have nonzero κ values and these are equal, the problem can be solved analytically, as in ref. 7.

1. Carlier, M. F. & Pantaloni, D. (1981) *Biochemistry* **20**, 1918–1924.
2. Carlier, M. F. (1982) *Mol. Cell. Biochem.* **47**, 97–113.
3. Wegner, A. (1976) *J. Mol. Biol.* **108**, 139–150.
4. Hill, T. L. & Kirschner, M. W. (1982) *Int. Rev. Cytol.* **78**, 1–125.
5. Pardee, J. D. & Spudich, J. A. (1982) *J. Cell Biol.* **93**, 648–654.
6. Mockrin, S. C. & Korn, E. D. (1982) *J. Cell Biol.* **95**, 284a (abstr.).
7. Hill, T. L. & Carlier, M. F. (1983) *Proc. Natl. Acad. Sci. USA* **80**, 7234–7238.
8. Carlier, M. F., Hill, T. L. & Chen, Y. (1984) *Proc. Natl. Acad. Sci. USA*, in press.
9. Carlier, M. F. & Pantaloni, D. (1982) *Biochemistry* **21**, 1215–1224.
10. Hill, T. L. & Chen, Y. (1978) *J. Chem. Phys.* **69**, 1126–1138.
11. Hammersley, J. M. & Handscomb, D. C. (1964) *Monte Carlo Methods* (Methuen, London).